A PROTOTYPE OF HYBRID SOLAR VEHICLE: SIMULATIONS AND ON-BOARD MEASUREMENTS

Adinolfi G.(**), Arsie I.(*), Di Martino R.(*), Giustiniani A.(**), Petrone G.(**), Rizzo G.(*), Sorrentino M.(*)

(*) DIMEC, (**) DIIIE
University of Salerno, 84084 Fisciano (SA), Italy
Phone: 01139089964080
Fax: 01139089964037
E-mail: msorrentino@unisa.it

The paper deals with the modeling, control and testing of a Hybrid Solar Vehicle (HSV) prototype. Vehicle set-up and instrumentation are accomplished at University of Salerno (UNISA), within an EU funded Leonardo project, starting from an existing electric vehicle. Suited experimental activities were performed to identify and validate a comprehensive model of the propulsion system resulting from the integration of a series hybrid powertrain with a photovoltaic (PV) array. Then, a simulation analysis was performed to address on-board energy management issues as well as assess prototype performance over a selected driving cycle.
Simulation results show that appropriate components sizing and supervisory control strategies concur in improving fuel economy significantly, up to 30 kilometers per liter of Diesel fuel.

Symposium topics: Advanced Concept Vehicle(21), Electric Vehicle, Hybrid Vehicle & Fuel Cell vehicle (22).

1. INTRODUCTION

Sustainable Mobility issues are gaining increasing attention both among specialists and in public opinion, due to the major impact of automotive systems on carbon dioxide production, climate changes and fossil fuel depletion. Recently, increasing efforts are being spent towards the application of solar energy to electric and hybrid cars. While solar vehicles do not represent a practical alternative to cars for normal use, the concept of a hybrid electric car assisted by solar panels appears more realistic [1].

In fact, thanks to a relevant research effort, in the last decade Hybrid Electric Vehicles (HEV) have evolved to industrial maturity, and represent now a realistic solution to important issues, such as the reduction of gaseous pollution in urban drive as well as the need for a substantial increase of energy conversion efficiencies. On the other hand, the use of solar energy on cars has been considered with a certain skepticism by most users, including automotive engineers. This may be due to the simple observation that the net power achievable in a car with current photovoltaic panels is about two order of magnitude less than maximum power of most of today cars. But a more careful analysis of the energy involved demonstrate that this perception may be misleading. In fact, there is a large number of drivers utilizing daily their car for short trips and with limited power demand [2]. In those conditions, the solar energy collected by solar panels on the car along a day may represent a significant fraction of the energy required for traction [3].

In spite of their potential interest, solar hybrid cars have received relatively little attention in literature. Some prototypes have been developed or are under current development [4]. Although these works demonstrate the general feasibility of such an idea, detailed presentation of results and performance, along with a systematic approach to solar hybrid vehicle design, seem still missing in literature.

Therefore, appropriate methodologies are required to address both the rapid changes in the technological scenario and increasing availability of innovative, more efficient components and solutions. A specific difficulty in developing a Hybrid Solar Vehicle relates to the many mutual interactions between energy flows, powertrain balance of plant and sizing, vehicle dimension, performance, weight and costs, whose connections are much more critical than in either conventional or hybrid electric vehicles. Moreover, the control strategies for HSV cannot be simply derived from the solutions developed for HEV. In fact, the presence of solar panels requires to extend the SOC management strategies also to parking phases, while the study of suitable control techniques is needed in order to maximize the net power from solar panels (MPPT). Finally, many HSV prototypes tend to adopt a series structure, while most of today HEV adopt a parallel or series/parallel approach. Series structure appears more suitable for plug-in hybrid applications [5], and is compatible with the use of in-wheel motors with built-in traction control and anti-skid [6]. Moreover, the series configuration represents a natural bridge towards the introduction of fuel cell hybrid vehicles.

This paper deals with the development of a prototype of Hybrid Solar Vehicle with series structure. This activity has been started in the framework of the UE funded Leonardo project "Energy Conversion Systems and Their Environmental Impact" [7], a project with research and educational objectives.

The paper is structured as follows: in section 2 the main technical specifications of the prototype are given along with a brief description of the series lay-out; then in section 3 the main submodels (i.e. electric motor, electric generator, lead-gel battery pack, AC-DC converter and solar panels) are presented and their experimental characterization discussed; section 4 reports on a simulation analysis conducted to assess actual vehicle performance and evaluate the fuel economy gains that can be achieved by optimizing both design and on-board energy management; in section 5 some preliminary on-board measurements are plotted and discussed; finally, the conclusion section ends the paper and also introduces on-going and future activities.

2. THE HSV PROTOTYPE

Table I lists the main features and specifications of the HSV prototype (see Fig. 1), now under-development at DIMEC-UNISA lab facilities.

Table 1 – Actual HSV prototype specifications.

Vehicle	**Piaggio Porter**
Length	3.370 m
Width	1.395 m
Height	1.870 m
Drive ratio	1:4.875
Electric Motor	**BRUSA MV 200 – 84 V**
Continuous Power	9 KW
Peak Power	15 KW
Batteries	**16 6V Modules Pb-Gel**
Mass	520 Kg
Capacity	180 Ah
Photovoltaic Panels	**Polycrystalline**
Surface A_{PV}	1.44 m^2
Weight	60 kg
Efficiency	0.125
Electric Generator	**Yanmar S 6000**
Power COP/LTP	5.67/6.92 kVA
Weight	120 kg
Overall weight (w driver)	
M_{HSV}	1950 kg

Vehicle lay-out is organized according to a series hybrid architecture, as shown on Fig. 2. With this approach, the photovoltaic panels PV assist the Electric Generator EG, powered by an Internal Combustion Engine (ICE), in recharging the Battery pack (B) in both parking mode and driving conditions, through the Electric Node (EN). The Electric Motor (EM) can either provide the mechanical power for the propulsion or restore part of the braking power during regenerative braking. In this structure, the thermal engine can work mostly at constant power, corresponding to its optimal efficiency, while the electric motor EM is designed to assure the attainment of the vehicle peak power.

Fig. 1 – The Hybrid Solar Vehicle Prototype.

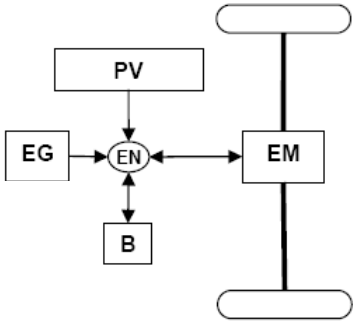

Fig. 2 –Scheme of the series hybrid solar vehicle.

3. HSV MODELING AND EXPERIMENTAL CHARACTERIZATION

HSV simulation, whose results are presented in Section 4, was performed by means of a longitudinal vehicle model developed under the following hypotheses: i) drag (C_x) and rolling (C_r) coefficients are assumed equal to 0.4 and 0.02, respectively; ii) the drag force is considered acting on vehicle centre of gravity; iii) overall transmission efficiency η_{tr} is set to 0.9; iv) rotational inertia is accounted for increasing vehicle weight by 10%, therefore effective mass M_{eff} equals 1.1 M_{HSV}. The resulting longitudinal model relates requested power at wheels to the road load, as follows:

$$P_w = W_{HSV} \cdot g \cdot v \cdot \left[C_r \cos(\alpha) + \sin(\alpha)\right] + 0.5\rho C_x A v^3 + \\ + Meff \frac{dv}{dt} v \qquad (1)$$

where α and v are the road grade and vehicle speed, respectively.

For non negative P_w values, the mechanical power requested to the EM is:

$$P_{EM} = \frac{P_w}{\eta_{tr}} \qquad if \quad P_w \geq 0 \qquad (2)$$

P_{EM} can also be expressed as function of power contributions coming from electric generator, battery and PV array, as follows:

$$P_{EM} = \eta_{EM} \left(P_{EG} \cdot \eta_{AC/DC} + P_B + P_{PV}\right) \quad if \quad P_w \geq 0 \qquad (3)$$

where P_x is the power supplied by the x component, η_{EM} is the EM efficiency and $\eta_{AC/DC}$ is the AC/DC converter efficiency, here set to 0.92. For the current application, a 3.3 kW battery charger will be coupled to the existing one, thus allowing to increase the power drawable from the electric generator up to 5.4 kW.

On the other hand, when $P_w<0$, the regenerative braking mode is active, resulting in the following expression for the electrical energy delivered by the EM:

$$P_{EM} = P_w \cdot \eta_{tr} \cdot \eta_{EM} \qquad if \qquad P_w < 0 \tag{4}$$

During regenerative braking, battery can be charged by EG and PV also, thus the following equation holds for negative P_w values:

$$P_B = P_{EM} - P_{EG} \cdot \eta_{AC/DC} - P_{PV} \qquad if \qquad P_w < 0 \tag{5}$$

3.1 Electric generator

The electric generator, is composed of a Diesel engine, one cylinder, 406 cm^3, coupled with a 3 phase synchronous induction machine. Experiments were carried out to map the efficiency of the electric generator in a wide operating region, accounting for the whole path from fuel to electrical power. The experimental set-up was arranged with a 3-phase pure resistive, balanced electrical load. The measurements were accomplished at constant engine speed (3000 rpm), corresponding to a 50 Hz electric signal, with regularly spaced variation of electrical load by steps of 600 W, up to 5400 W. Fig. 3 shows the experimental EG efficiency vs. the output power of the electrical generator (EG). The efficiency was detected by processing the measurements of fuel consumption and output voltage and current, as follows:

$$\eta_{EG} = \frac{P_{EG}}{\dot{m}_f H_i} = \frac{V \cdot I}{\dot{m}_f H_i} \tag{6}$$

In Fig. 3 the efficiency predicted by a black box model identified vs. the experimental data is also plotted. The model expresses the overall efficiency of the electric generator as function of the output electrical power by a 4th order polynomial regression.

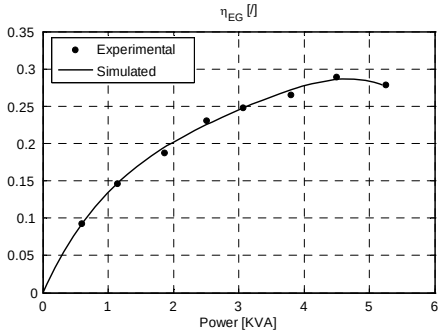

Fig. 3 – Comparison between experimental and predicted electric generator efficiency.

3.2 PV array

The PV array, which was placed on vehicle roof as shown on Fig. 1, has been characterized by connecting the converter output to a resistive load in order to exploit it as a varying resistance.

Performance data for the PV array have been collected by means of a National Instruments Compact RIO 9004 system. Figs. 4 and 5 show the results of the PV roof experimental characterization in both uniform irradiation level and mismatched conditions. The comparison with simulated data indicates the satisfactory accuracy in reconstructing output power vs. PV array voltage. Further details about PV array modeling can be found in [8].

The results shown in Fig. 4 also indicate that net PV efficiency sets around 10%. On the other hand, converter efficiency reaches its maximum value (i.e. 85%) at about 35V, namely at the input voltage level corresponding to the maximum power delivered by the PV array. This is encouraging, because the boost converter will be controlled in such a way as to ensure high voltage and efficiency operations. Specifically in this activity, as the main goal is to maximize solar energy caption during parking rather then in driving phases, the Perturb and Observe MPPT algorithm, developed by the authors for stationary applications, will be implemented.

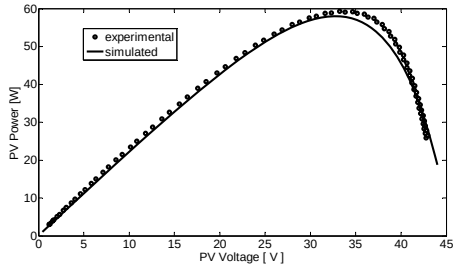

Fig. 4 – Comparison between simulations and experiments under uniform irradiation level: whole PV field (390W/m2).

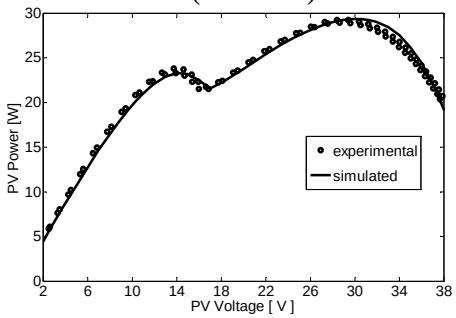

Fig. 5 – Experimental measurements and simulated characteristics of the PV roof in mismatched conditions.

Regarding the PV energy contribution to vehicle traction, it was computed on the basis of real energy measurements collected on a stationary PV plant located within UNISA area. Fig. 6 shows the histogram of the daily average energy throughout 2007. This distribution results in the following daily average evaluated on a year basis:

$$E_{sun,day} = 3.1 \qquad \left[\frac{kWh}{kWp\ day}\right] \tag{7}$$

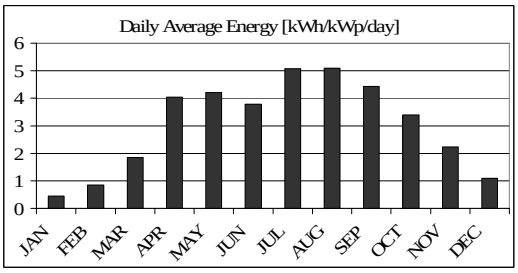

Fig. 6 – 2007 distribution of daily average energy generated by a stationary PV plant located within UNISA area.

Considering the PV roof efficiency of 10%, a

nominal power of 1kW can be obtained with a 1/0.1=10 m^2 array. Therefore, daily average energy yielded by the 1.44 m^2 PV roof (see Table 1) can be estimated as follows:

$$E_{PV} = E_{sun,day} \cdot \frac{A_{PV}}{10} = 3.1 \cdot \frac{1.44}{10} = 450 \quad [Wh/day] \qquad (8)$$

Another key aspect currently under investigation regards the battery charger connected to the PV roof. Battery charging optimization is one of the most challenging issues in any hybrid vehicle. This because not only a very high efficiency energy conversion is needed, but also the best management of the battery pack is required in order to make its lifetime the longest possible.

As for the efficiency, the main design issue is related to the intrinsic variability of the solar source of energy, with significant variations in irradiation levels along the day that dramatically affect the switching converter input power level and, consequently, its efficiency. To this regard, classical design techniques usually consider the highest irradiation level (e.g. 1kW/m^2) as a reference value for the converter design, but this assumption might lead to poor performances at lower irradiation levels, with an unsatisfactory amount of energy produced in early morning and late afternoon as well as during cloudy days.

As for the battery pack charging strategy, the best solution is represented by multi-output dc-dc converters [10], with each output devoted to a single battery module or a small group of them. Best performances in terms of charge equalization are ensured by flyback-based topologies, since a simple set of a secondary winding, a diode and a capacitor is devoted to charging a battery unit.

A prototype of such a dc-dc solar battery charger is going to be realized on the basis of a suitable design procedure that accounts for solar irradiation variation, through the concept of energy – and not power – efficiency. In Fig. 7 and Fig. 8 a preliminary Pareto front obtained by a multi-objective optimization accounting for energy efficiency and size is shown: it compares the optimal design solutions with a standard solution suggested in literature. It is evident from the energy plots that the proposed converter gives a better efficiency profile throughout the day.

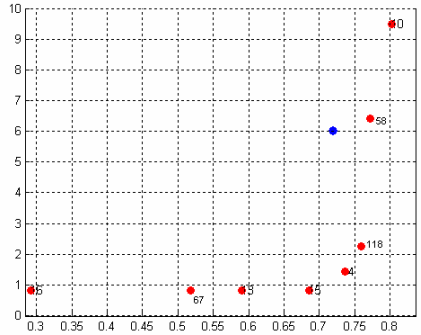

Fig. 7 – Comparison among the Pareto front obtained by means of the proposed design method (red dots) and the classical approach (blue dot) [11]: horizontal axis=efficiency (/), vertical axis=size (cm^3).

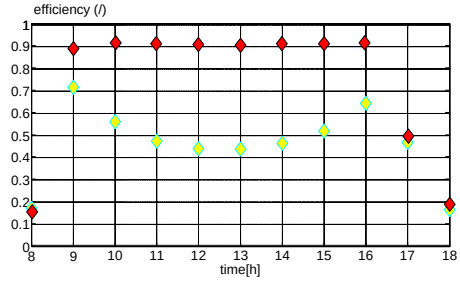

Fig. 8 – Comparison of energy efficiencies for standard design approach (yellow) and the design method under study (red).

3.2 Battery pack

The battery pack model estimates battery state of charge (SOC), current and thermal state as function of the actual electrical power (i.e. positive in discharge and negative in charge). The actual current is computed starting from the electrical power, by applying the Kirchoff's law to the equivalent circuit shown on Fig. 9.

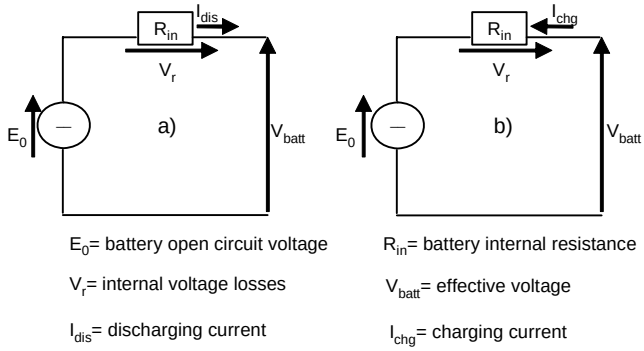

Fig. 9 – Equivalent circuit of the battery pack [a) discharge; b) charge].

The internal resistance R_{in} was modeled, following the approach proposed by [12], as a nonlinear function of battery temperature and state of charge. Fig. 10 focuses on the effect of SOC, showing high charge and discharge resistance at high and low SOC, respectively.

The battery model accuracy was checked by comparing simulated data with experiments conducted both in case of battery discharging and charging (see Fig. 11). The agreement between experiments and model outputs confirms the validity of extending the model proposed by [12] to the battery pack the HSV prototype is equipped with. It is worth mentioning that the data shown in Fig. 11 refer to initial SOC values of 1 and 0.6 for battery discharging and charging, respectively.

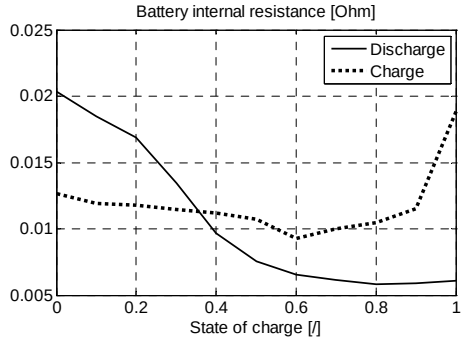

Fig. 10 –Variation of battery internal resistance in charging and discharging as function of SOC [12].

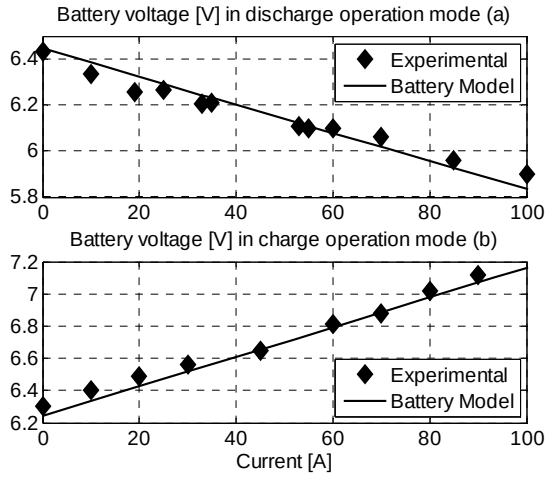

Fig. 11 – Comparison between model [12] and experimental data collected during battery discharging and charging.

3.4 Electric motor

The efficiency of the electric motor (EM) is simulated by a black box model identified vs. the technical data sheets provided by motor manufacturer. The model expresses the efficiency as function of the mechanical power provided for the propulsion via a 3rd order polynomial regression.

Figure 12 shows both experimental and simulated efficiency vs. provided power.

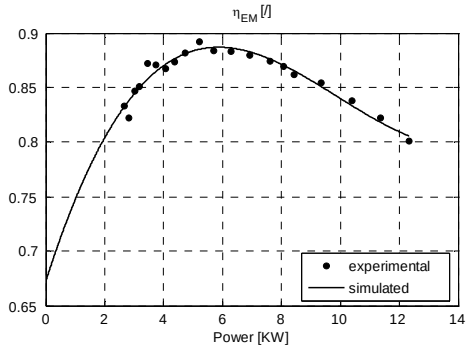

Fig. 12 – Comparison between experimental and predicted electric motor efficiency vs. provided power.

4. HSV SIMULATION

In order to assess the HSV prototype performance not only at the current developmental stage, but also analyzing two further scenario of improved vehicle configurations, a simulations analysis was performed. Such an analysis was accomplished by solving, in a backward manner, the longitudinal vehicle dynamics (i.e. Eq. 1) for a driving cycle composed of 4 ECE cycles, as the one shown on Fig. 13.

An intermittent scheduling of the Diesel engine powering the electric generator was imposed. Such a strategy was set-up by solving a constrained optimization problem, aimed at defining the number of engine starts and corresponding timing and duration that guarantee a day through charge sustaining strategy. For further details about the aforementioned optimization analysis, the reader is addressed to previous contributions [13, 14].

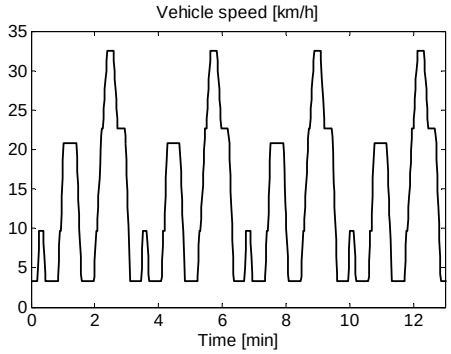

Fig. 13 – Module of ECE driving cycle.

Table 2 summarizes the results obtained in the three analyzed scenarios.

The results reported in Table 2 indicate that an acceptable fuel economy can be obtained even with current vehicle configuration. This is possible thanks to the high efficient use of the Diesel engine addressed by the optimized control strategy described above. Particularly, Fig. 14.a shows that the Diesel engine is turned on once, after 15 minutes, delivering 5 kW to battery and/or EM for about 25 minutes. This allowed to operate the EG itself at an overall efficiency as high as 0.28 (see Fig. 3). The EG energy contribution caused battery to partially recover the state of charge reduction occurred in the first part of the driving cycle, resulting in a final SOC of 0.732, as shown on Fig. 14.b.

The difference between initial and final state of charge was actually imposed in the control optimization task. Such a choice ensures the energy captured by PV array during parking be stored in the batteries, while maintaining a day through charge sustaining strategy.

Table 2 – Results of HSV simulation.

Scenario	1	2	3
Fuel economy (km/liter)	15.18	21.70	29.15

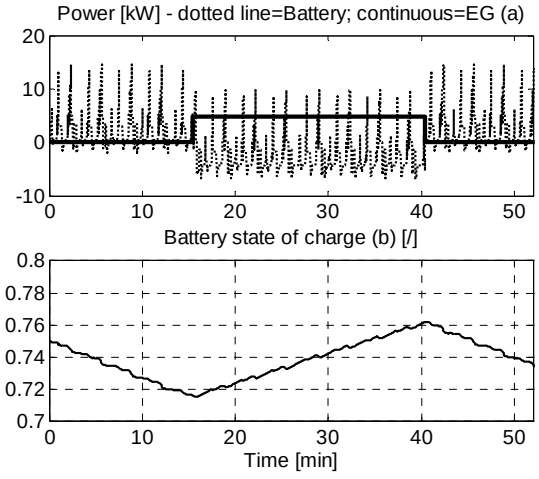

Fig. 14 – Battery and EG power trajectory (a). Battery state of charge (b).

Regarding the other scenarios, it is worth mentioning here that the second scenario corresponds to an optimized vehicle configuration, in which a 0.18 efficient PV array (i.e. E_{PV} = 810 Wh/day) replaces the actual one and battery capacity is lowered down to 75 Ah. The latter hypothesis takes into account the impact

of vehicle hybridization, as the added electric generator allows to reduce both battery storable energy and nominal power. The lower battery capacity also causes the weight to decrease form 1950 kg to 1658 kg. Such a configuration results in a fuel economy improvement up to 22 km/liter, as indicated in Table 2. Finally, the third scenario was considered to account for a further weight reduction (by 20 %), obtainable both by improving vehicle materials [3] and switching to a lighter battery typology, such as lithium batteries. The simulated fuel economy in this case gets close to 30 km/liter.

5. ON-BOARD MEASUREMENTS

Some preliminary on-board measurements were performed. Fig. 15 shows EM torque and vehicle speed, respectively sensed by a torsiometer and an optical proximity sensor. These devices interface with a data acquisition system developed in Lab-view environment and processed by a cRIO 9004 programmable controller. Such a cRIO controller is currently under further development to include current and voltage measurements as well as digital I/O, with the final aim of performing both on-board energy monitoring and supervisory control of the HSV prototype.

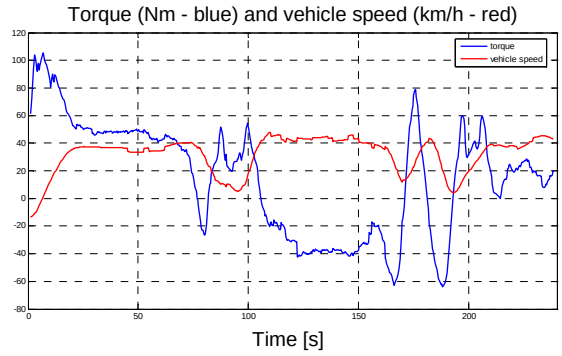

Fig. 15 – On-board measurement of EM torque and vehicle speed.

6. CONCLUSION

The paper reported on the actual developmental stage of a hybrid solar vehicle prototype. The experimental and numerical activities conducted to develop and validate a comprehensive HSV model were presented. The model accounts for vehicle longitudinal dynamics along with the accurate evaluation of energy conversion efficiency for each powertrain component.

Actual vehicle performance and fuel economy were analyzed by simulating the HSV prototype on a driving route composed of 4 ECE cycles. The resulting fuel consumption was 15 km/liter. Further simulations showed that fuel economy can be increased up to 30 km/liter both by substituting the actual PV array with more advanced solar technology and by appropriately resizing HSV components.

On-going and future activities focus on numerical, experimental and prototype developmental tasks. Particularly, the optimal EG scheduling will be the subject of future optimization analyses, which will aim at maximizing fuel economy while guaranteeing a day through charge sustaining operation in different driving conditions. In parallel, suited on the-road test and measurements will be performed to validate both simulation results and control strategies effectiveness. Regarding prototype improvements, the installation of an automated sun-tracking roof to further enhance solar energy captation is under current study.

REFERENCES

[1] Neil C., 2006, "Solar Hybrid Vehicles", Energy Pulse, available at www.energypulse.net.

[2] Statistics for Road Transport, available at www.statistics.gov.uk/CCI/nscl.asp? ID=8100.

[3] Arsie I., Marotta M., Pianese C., Rizzo G., Sorrentino M., 2005, "Optimal Design of a Hybrid Electric Car with Solar Cells", Proc. of 1st AUTOCOM Workshop on Preventive and Active Safety Systems for Road Vehicles, Istanbul, Sept.19-21.

[4] Fiat Phylla, 2008, www.motorauthority.com/cars/fiat/fiat-phylla-concept-previews-new-topolino-electric-minicar/.

[5] Letendre S., Perez R., Herig C., 2003, "Vehicle Integrated PV: A Clean and Secure Fuel for Hybrid Electric Vehicles", Proc. of the American Solar Energy Society Conference, June 21-23, Austin,TX.

[6] www.itee.uq.edu.au/~serl/UltraCommuter.html.

[7] Leonardo Program "Energy Conversion Systems and Their Environmental Impact", http://www.dimec.unisa.it/leonardo.

[8] Petrone, G., Spagnuolo, G., Vitelli, M., 2007, "Analytical model of mismatched photovoltaic fields by means of Lambert W-function", Journal of Solar Energy Materials and Solar Cells, Vol. 91, Issue 18, pp. 1652-1657.

[9] Petrone, G., Femia, N., Spagnuolo, G., Vitelli M., 2005, "Optimization of perturb and observe maximum power point tracking method", IEEE Transactions on Power Electronics. Vol. 20, pp. 963-973.

[10] Park, H.S., Kim, C.E., Moon, G.W., Lee, J.H., Oh:, J.K., 2007, "Two-Stage Cell Balancing Scheme for Hybrid Electric Vehicle Lithium-Ion Battery Strings", IEEE Power Electronics Specialists Conference, 17-21 June 2007, pp: 273-279.

[11] Sclocchi, M., "Switching power supply design, continuous mode flyback converter", available at www.national.com/appinfo/power/files/flyaback-cont2000-5000-new.pdf.

[12] Burch, S., Cuddy, M., Johnson, V., Markel, T., Rausen, D., Sprik, S., and Wipke, K., "ADVISOR: Advanced Vehicle Simulator", available at http://www.avl.com/advisor.

[13] Arsie I., Rizzo G., Sorrentino M., 2007, "Optimal Design and Dynamic Simulation of a Hybrid Solar Vehicle" SAE paper 2006-01-2997, SAE Transactions – Journal of Engines, vol. 115-3.

[14] Arsie, I., Di Martino, R., Rizzo, G., Sorrentino, M., 2007, "Supervisory Control of a Hybrid Solar Vehicle Prototype", Proc. of the 5th IFAC Symposium on Advances in Automotive Control, Monterey (CA, USA) August, 20-22.